Cheraitia et al., 2015

Volume 1 Issue 1, pp.259-274

Year of Publication: 2015

DOI-https://dx.doi.org/10.20319/mijst.2016.s11.259274

This paper can be cited as: Cheraitia, K., Lounis, Mehenni, M., Azzaz, M., & Osmane, K. (2015). Neutron Activation Analysis of ND-FE-B Magnet and Determination of the Content of ND after Oxalate Precipitation and Production of ND_2O_3. MATTER: International Journal of Science and Technology, 1(1), 259-274.

NEUTRON ACTIVATION ANALYSIS OF ND-FE-BMAGNET AND DETERMINATION OF THE CONTENT OF ND AFTER OXALATE PRECIPITATION AND PRODUCTION OFND_2O_3

K. Cheraitia
Laboratory of Sciences and Material Engineering, University of Sciences and technology Houari Boumediene, BP32 El Alia 16111 Algiers, Algeria
cheraitiak@yahoo.fr

Lounis
Laboratory of Sciences and Material Engineering, University of Sciences and technology Houari Boumediene BP32 El Alia 16111 Algiers, Algeria
zlounis@yahoo.com

M. Mehenni
Laboratory of Sciences and Material Engineering, University of Sciences and technology, Houari Boumediene BP32 El Alia. 16111 Algiers, Algeria

M. Azzaz
Laboratory of Sciences and Material Engineering, University of Sciences and technology, Houari Boumediene, BP32 El Alia 16111 Algiers, Algeria

K. Osmane
Laboratory of Sciences and Material Engineering, University of Sciences and technology, Houari Boumediene, BP32 El Alia. 16111 Algiers, Algeria

Abstract

In practice, the properties of the neodymium magnets are highly dependent on the precise composition of the alloy and its microstructure. The aim of our work is to determine the content of neodymium and the impurities of a magnet Nd-Fe-B. The first step is to analyze the impurities from a super Nd-Fe-B magnet. We used the following techniques: The neutron radiography, the neutron activation analysis (NAA) and the scanning electron microscope coupled with EDX. The samples of Nd-Fe-B and standards are weighed and packed in polyethylene envelopes. They are simultaneously irradiated in thermal reactors column (NUR Draria-Algiers) under a neutron fluxof3.4x10^{12}n/cm^2/s. The radio activity of the samples is measured using a spectrometry chainγ (hyper pure germanium detector Hp/Ge). Gamma (γ)spectrum is presented in the energy range between 100keV and 2000keV. The detected elements are: Ni, Al, Ti, Cu, Mn, In, Ta, Ce, Sm, Eu, Np, Yb, Gd, and Lu. The digital processing of the images obtained by the neutron radiography shows that in the Nd-Fe-B matrix, the distribution of elements is homogeneous. The SEM micrographics show three different phases of contrasts: light, gray and black which correspond to Nd, Fe, and B. In a second step the powder is dissolved in hydrochloric acid solution. We add an oxalic acid solution to precipitate Nd as neodymium oxalate. The identification of the most intense peaks in the XRD spectrum shows the presence of a single compound which hydrated neodymium oxalate chemical formula $Nd_2(C_2O_4)_3.10H_2O$. Its purity is measured by neutron activation analysis. The counting of γ spectrum shows that the purity of the precipitate is higher than 99%. Then, the thermal decomposition transforms this powder to neodymium oxide. After the reduction we obtain pure neodymium. The analytical balance shows that this magnet contains 26% ofneodymium.

Keywords

Analysis, Magnet, Neutron activation analysis (NAA), Neutron radiography, SEM-EDX, Precipitation chemical

1. Introduction

The rare earth elements include 17 chemical elements (metal), this group consists of 15 lanthanides and yttrium and scandium. Lanthanum and the lanthanides form a series whose chemical properties are very similar, which also commonly refers as " rare earth ": scandium

(38Sc), yttrium (39Y), lanthanum (57The) cerium (58EC), praseodymium (59Pr), neodymium (60Nd), promethium (61Pm), samarium (62Sm), europium (63Eu), gadolinium (64Gd), terbium (65Tb), dysprosium (66Dy), holmium (67Ho) erbium (68er), thulium (69Tm), ytterbium (70Yb), lutetium (70Lu). With the development of the nuclear industry and the development of new separation techniques (ion exchange, solvent extraction) lanthanides compounds have become more common chemicals. The Lanthanides are considered important industrial materials by their specific characteristics.

The specificity of rare earth is mainly due to the f electrons which gives them two essential properties: optical and magnetic. Their magnetic properties, which depend on quantum characteristics, are exceptional: the f electrons are not involved in chemical bonds; they are free to participate in magnetism.

The rare earths are used to make magnetic alloys (neodymium-doped dysprosium) which play an important role in advanced technologies used in particular for wind turbines. The rare earth having these f electrons are difficult to separate because their numbers of electrons also affect their physical properties, which has an impact on their industrial interest (Zakotnik et al., 2008; Milmo, 2010). The demand for rare earth elements increases wish 9-15% per year (Itakura et al., 2005, Zakotnik et al., 2007). Rare earths have exceptional magnetic properties, their saturation magnetization is much higher than the iron one (Ruoho, 2011).

From raw material the composition is very complex. The steps that achieve different lanthanides as pure products are long, difficult and expensive (Mokili & Potrenaud, 1996; Saito et al., 2006; Kanazawa & Kamitani, 2006; Lalleman et al., 2011). The dissolved lanthanides are separated from impurities by various reactions as the insolubility hydroxides, fluorides, oxalates, phosphates or alkali double sulfates (Yantasee et al, 2009; Duan et al., 2010; Moldoveanu & Papangelakis, 2012). In this context we would like to assess the degree of contamination of the magnet Nd-Fe-B. They have the highest magnetic field intensity. The production of neodymium (Nd) has considerably increased since the development of neodymium-iron-boron (Nd-Fe-B) permanent magnet (Du & Graedel, 2011; Rademaker et al., 2013). These magnets are found in almost all the NTIC products (New Technologies of Information and Communication). NTIC products whose life cycle does not usually exceed three years have become consumables. Just like the hard disks drive (HDD) in a personal computer, which contain neodymium and praseodymium

(Okabe, Takeda, Fukuda & Umetsu, 2003). The concept of sustainable development is invoked as a necessity for recycling materials. The waste from NTIC products has nevertheless a residual material value, compromised by the disassembly cost in the developed countries, but economic in developing or third worldcountries.

The aim of our work is to determine the content of neodymium and the impurities of a magnet Nd-Fe-B. Few studies mention the analysis of impurities in the magnets marketed. The first step is to analyze the impurities from a super Ned Feb. magnet. We used the following techniques:

The neutron radiography, the neutron activation analysis (NAA) and the scanning electron microscope coupled with EDX. In a second step the powder (Ned-Fe-B magnet) is dissolved in hydrochloric acid solution. We add an oxalic acid solution to precipitate Nd as neodymium oxalate (Mokili & Potrenaud, 1996, Kobayashi, Morita and Kubota, 1988). The powder was analyzed by X- ray diffraction. The gamma (γ) counting allows the determination of the content of neodymium, after oxalate precipitation and production of the Nd_2O_3 powder (Lyman & Palmer, 2011).

2. Experimental

Neutron activation analysis

The neutron activation analysis is a method of making a sample radioactive by irradiation in a neutron field and thereafter one proceeds to identification via the energy emitted by the corresponding isotopes and their half life (Wispelaere et al., 1973). Samples of the Nd-Fe-B matrix and the standard were weighed, packaged, and irradiated simultaneously in the thermal reactor column under a neutron flux magnitude of $5.4x10^{12}n/cm^2/s$. The long irradiation was made in thermal column, with a magnitude of $2.1x10^{11}n/cm^2$ /s for a time of 10 hours. At the end of the long irradiation, the samples were transferred directly to a shielded cell for 10 days decay time. The radioactivity of the samples was measured using a γ spectrometric chain which is composed of the following elements: germanium high purity detector (Hp/Ge) having a efficiency ε = 1.2%, and resolution of 1.80 keV. The ratio Pic/Compton is 40. These characteristics are measured for γ line at

1.33 MeV 60Co. A preamplifier and an analyzer 8192 ORTEC channels incorporating an amplifier samples and standard were measured in the same counting geometries.

Neutron radiography

This technique is non-destructive analysis for the control and structural characterization of opaque or solid materials at the micrometer scale. In this work, we will apply the so-called transfer technique to obtain radiographs of super magnet, thereafter we will use digital processing techniques of the images obtained for qualitative operation to access information structures. In the transfer method only the converter is exposed to neutron beams and becomes radioactive. The intensity of the secondary radiation is proportional to the spatial neutron intensities.The converter is transferred after irradiation in the dark room and placed in contact with a radiographic film. In this technique the gamma flux present in the beam does not interfere with the method.

Mass Spectrometry

A small portion of the sample is transformed into ions. These ions are then subjected to electric and possibly magnetic fields and their path will depend on the m/z ratio. After separation, the ions finish their path in a detector sensor. An analysis of the chemical composition of the samples was performed using a mass spectrometer SPECTRO MaxX.

Precipitation of neodymium

The precipitation tests were performed according to a planning of experiments at three levels 3^3. We have 27 experiments to be performed with three variables: the concentration of Nd, 0.001M, 0.003M, and 0.009M; The oxalic acid concentration of 0.5M, 1M and 0.75M and the pH of the solution 2.5, 3 and 3.5.

Characterization

The resultant powder was characterized by using X-ray diffract meter carried out with X' Pert Pro MPD under Cu-Kα radiation (λ=0.154 nm). Microstructure and chemical composition of the samples were investigated by JSM-6360, JEOL scanning electron microscope (SEM) equipped with an energy dispersive X-ray (EDX) analyser at an accelerating voltage of 10-20 kV.

3. Results and discussion

The results of neutron activation are presented as intensity spectra of γ radiation as a function of energy. The methodology adopted in this work is to identify all the elements present in the sample. This step is very important because it allows us to identify short period elements. These elements become saturated quickly and therefore they require very short irradiation time.

The long- period elements slowly reach saturation; they require higher fluency neutron irradiation. The qualitative analysis of elements is performed by short period's γ spectrometry. Inducedactivityinthesampleisduetoradioisotopeproduction.WhenN_1stableatomsofa materials are irradiated by a neutron flux φ (n/cm^2/s) for a time dt, the number of radioactive atoms N_1 formed is given by the (equation 1). At the same time begin the disappearance decay of radioisotopes formed. The system of evolution equations is obtained by producing the balance production – disappearance (equation 2).

$$dN_1 / dt = \sigma_1.\varphi.N_1 \quad (1)$$

$$dN_2/dt = \sigma_1.\varphi.N_1 - \sigma_2.\varphi.N_2 - \lambda_2 N_2 \quad (2)$$

Where:

- σ_i (cm²) the capture cross section of the radioisotope
- N_1 et N_2 (at/cm^3): density numbers respectively of the isotopes X_1 andX_2
- λ_i (s^{-1}): constant of radioactive decay of the radioisotopei
- φ(n/cm²/s): neutronflux
- *t* (s): neutron irradiation time

With the following conditions at t=0, N_1 (0) = N^0 and N_2 (0) =0, the solution of the system of

equations (1) and (2) is written:

$$N_1(t) = N_1^0 e^{-\sigma_1 \varphi . t} \quad (3)$$

$$N_1^0 = \frac{m.\xi.\mathrm{N}}{M_A} \quad (4)$$

Where:

- m: mass of the sample
- N: Avogadro's number
- M_A: atomicmass,
- ξ: istopicenrichment

$$(5)\ N_2(t) = \frac{\sigma_1.\varphi.N_1^0}{\lambda_2 + (\sigma_1 - \sigma_2)\varphi}(e^{-\sigma_1.\varphi.t} - e^{-(\lambda_2+\sigma_2.\varphi)t})$$

The activity $A_2(t)$ is written:

$$A_2(t) = \lambda_2.N_2(t) \qquad (6)$$

$$A_2(t_i) = \frac{\lambda_2\sigma_1.\varphi.N_1^0}{\lambda^* - \sigma_1.\varphi}(e^{-\sigma_1.\varphi.t_i} - e^{-\lambda^* t_i})$$

Asking $\lambda_{*.} = \lambda_2.N_2 + \sigma_2.\varphi$ equation (6) is written:

(7)

This relation is valid in most cases. However when it comes to a long irradiation for the elements with a large cross sections of absorption (high neutron flux), then take into account the consumption of target (burn-up).

For items with a large full resonance, consideration should account the fraction of the neutron spectrum located beyond the thermal field. The term $\sigma_1\varphi$ will be replaced by ($\sigma_1\varphi+I_0.\varphi_{epi}$)

Where:

- φ_{epi} is the epi-thermal neutron flux and I_0, the resonance integral (in barns).

The sample activity at the end of irradiation (at time t = t_i) and after a time decrease t_d is

given by equation (8).

$$A(t,t)=A(t)e^{-\lambda_2 t_d} \qquad (8)$$

The cumulative activity of the sample after a time t_c count is:

$$(9)\ A_2(t_i,t_d,t_c)=\int_0^{t_c} A_2(t_i,t_d)e^{-\lambda_2 t_c}dt$$

$$(10)\ A_2(t_i,t_d,t_c)=\frac{\sigma_1.\varphi.N_1^0}{\lambda_2}(1-e^{-\lambda_2 t_i})(1-e^{-\lambda_2 t_c})e^{-\lambda_2 t_d}$$

Determining the individual half-life of each radioelement is made by following the decrease of this one at constant time intervals. Table 1 provides the nuclear reactions used for sample analysis. The presence of specific radioisotopes is demonstrated in the γ spectra (Figures1-4).

Table 1: *Nuclear reactions for sample analysis*

Element	**Target isotopes**	**Nuclear reactions**	**product**	**ε (%)**	**λ (s^{-1})**	**γ peak (KeV)**
Nd	^{146}Nd	^{146}Nd (n, γ) ^{147}Nd	^{147}Nd	17.2	7.30E-07	531
Fe	^{58}Fe	^{58}Fe (n, γ) ^{59}Fe	^{59}Fe	0.28	1.68E-07	1099
Co	^{59}Co	^{59}Co (n, γ) ^{60}Co ^{61}Ni (n, p) ^{60}Co	^{60}Co	100	3.79E-09	1173
Al	^{28}Al	^{28}Al (n, γ) ^{29}Al	^{29}Al	100	4.68E-03	1780
V	^{51}V	^{51}V (n, γ) ^{52}V	^{52}V	99.75	2.8E-03	1435
Cu	^{63}Cu	^{63}Cu (n, γ) ^{64}Cu	^{64}Cu	69.15	1.36E-05	511

For the three energy intervals (Figure 1) we can clearly infer the existence of elements that accompany Fe and Ned, these are: Al28, V52, Mn56, Cu66, Ge66, Ag108, Cs 136, Lu177m, Tb160, Re224, Bk246. Note also the presence of rare earth elements such as Dy160 and its isotope Dy165. The elements of long period require very large irradiation time and do not appear on these spectra. The time counting of the vanadium element is taken as the reference time. The time decay of the respective elements will be determined from time decay vanadium which is given in table 2.

Table 2: *Reference time of the elements analyzed by NAA*

Element	**Decay time (s)**
Vanadium	0
Cooper/Manganese	9035
Neodymium	18585
Iron	91534
Nickel	100219
Nd-Fe-B Matrix	169477
Cobalt	176891

The energy measured by the neutron activation technique is confirmed by tables and energy isotopes. Tables 3 and 4 show the ratios of the matrix Nd-Fe-B obtained by neutron activation analysis, where all the elements short and long periods present appeared.

Table 3: *Elements present in the Nd-Fe-B matrix after 2Min of a decay time*

Probable radioisotope	**Energy measured**	**Probable radioisotope**	**Energy measured**
Ti-51	242	Lu-177m	54.07
Ni-65	55	Sm-153	69.67
Ni-65	181	J-131	80.18
In-116m	92	Eu-155	86.54

Ni-65	39	Cd-109	88.03
Cu-64	274	Nd-147	91.11
Ti-51	14	Np-239	99.55
Ni-65	24	Ta-182	100.11
In-116m	818.70	Sm-153	103.18
Mg-27	843.76	Gd-153	103.18
Mn-56	846.77	Np-239	103.76
Ni-65	852.70	Eu-155	105.31
Ti-51	928.63	Lu-177m	105.36
Ni-65	952.99	Np-239	106.12
In-116m	1096	Lu-177m	112.95
Cu-64	1346.55	Np-239	117
V-52	1434	Se-75	121.12
K-42	1523	Eu-152	121.78
Al-28	1778	Eu-154	123.07
Mn-56	1810.67	Ba-131	123.84

Table 4: *Elements present in the Nd-Fe-B matrix after 10 days of a decay time*

Probable radioisotope	**Energy measured**	**Probable radioisotope**	**Energy measured**
Lu-177m	54.07	Ba-131	123.84
Sm-153	69.67	Yb-175	282.52
J-131	80.18	Pa-233	300.04
Eu-155	86.54	Se-75	303.92
Cd-109	88.03	Nd-147	319.41
Nd-147	91.11	La-140	432.49
Np-239	99.55	Nd-147	439.88
Ta-182	100.11	Hf-181	482.18

Sm-153	103.18	Ru-103	497.33
Gd-153	103.18	Cs-134	561.76
Np-239	103.76	Ga-72	600.95
Eu-155	105.31	Sc-46	889
Lu-177m	105.36	Tb-160	966.44
Np-239	106.12	Rb-86	1078
Yb-169	109.78	Ta-182	1121

The images obtained by neutron radiography are presented below in the (Figure 5). The difference in contrast is due to the presence of the elements in the matrix Fe-Nd-B that does not absorb neutrons. We note that there are two colors, a dark which represents the clear film and the other representing the Fe-Nd-B matrix. The distribution of the components of the matrix is said to be homogeneous because the light portion of image shows that there is no chaotic distribution of these elements.

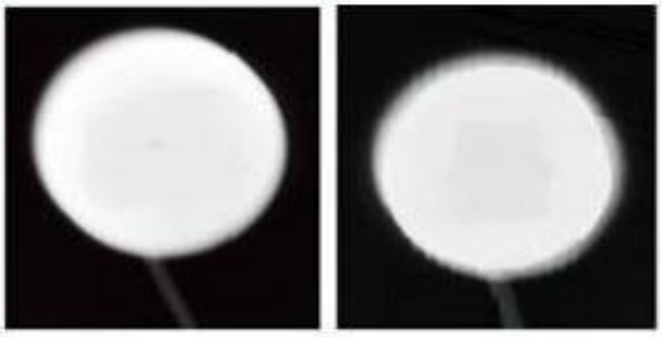

Figure 5: *Neutron radiography image of the Nd-Fe-B Matrix*

(a)100-500Kev. (b) 500-1200Kev.(c)1200-1900Kev.

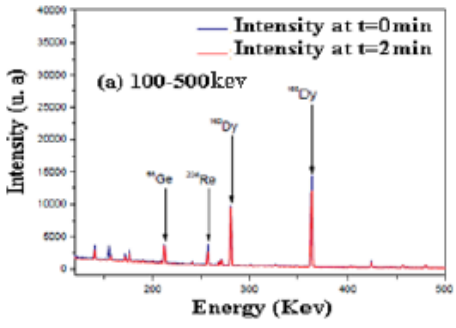

Figure 1: *Gamma specta of the Nd-Fe-B Matrix: (a)100-500Kev. (b)500-1200Kev. (c)1200-1900Kev.*

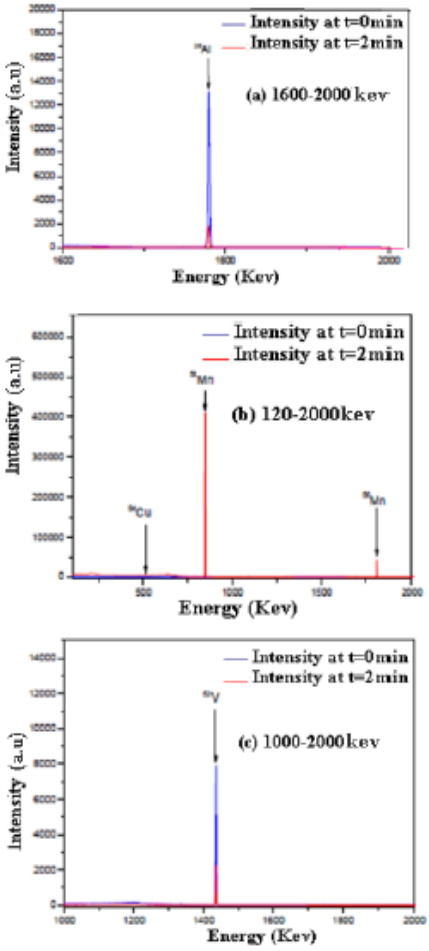

Figure 2: *Gamma specta of the standard sample: (a)1600-2000Kev. (b)120-2000Kev. (c)1000-2000Kev.*

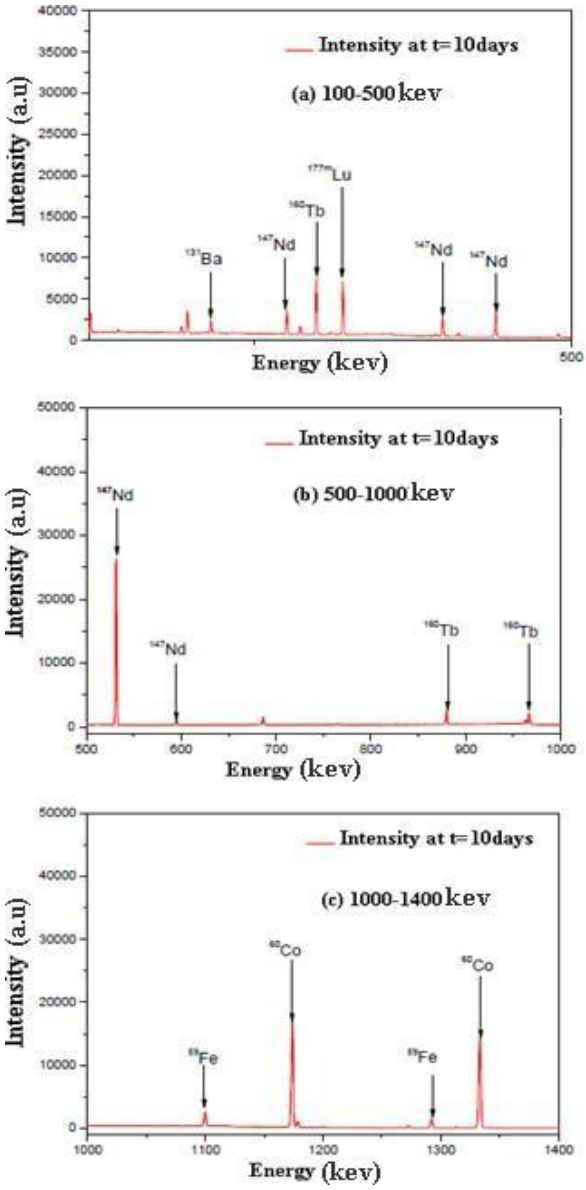

Figure 3: *Gamma specta of the Nd-Fe-B Matrix: (A) 100-500Kev. (b) 500-1000Kev. (c) 1000-1400kev*

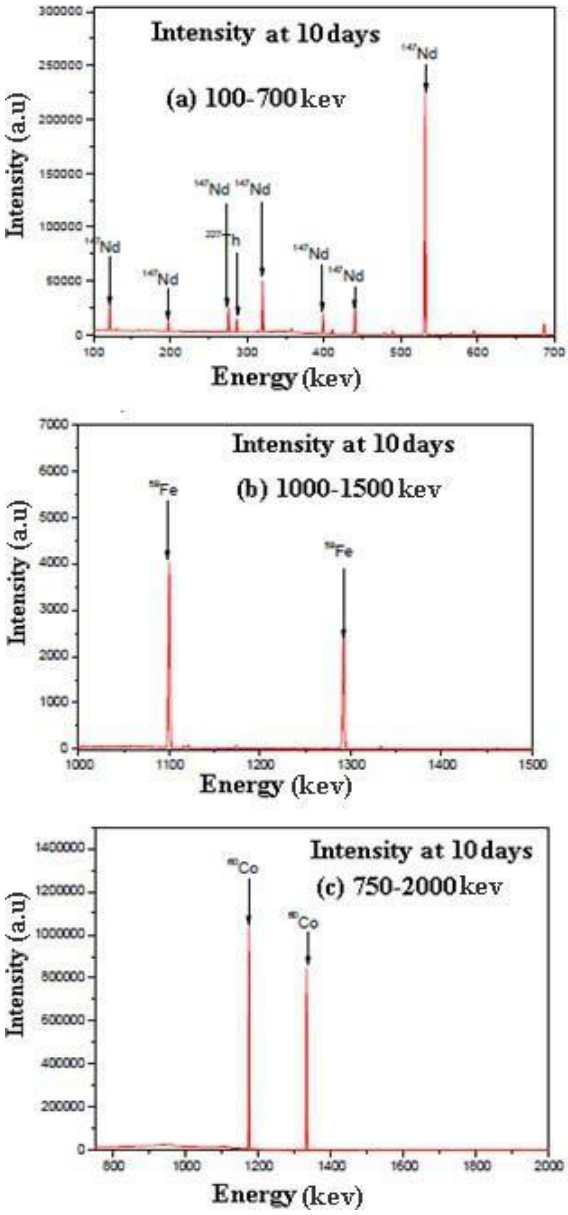

Figure 4: *Gamma specta of the standard sample: (A) 100-700Kev. (b) 100-1500Kev. (c) 750-2000kev*

The micrographs (Figure 6), shows the microstructure of Fe-Nd-B matrix, we can see the distribution of three different phases of contrast clear, gray, and black representing the iron, the neodymium and the boron. It is observed that the distribution of components is typical of a matrix of sintering materials. Neodymium grains are distributed between iron particle interstices. The particle distribution is uniform over the entire sample surface.

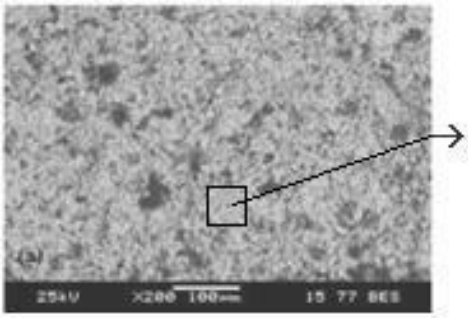

Elements	Wt %	At%
SiK	1.23	3.04
Pr	7.92	3.90
Nd	26.21	12.63
Fe	64.64	80.43

Figure 6: *Energy dispersive X-ray spectroscopy of the Nd-Fe-B Matrix*

On the results of the precipitation tests: the best yield, 99% was obtained for [Nd]

=0.003M, pH=3 and an oxalic acid concentration of 0.75M.

The obtained precipitate (neodymium oxalate) is analyzed: Identification of the three intense peaks of spectrum XRD (Figure 7) with cards ICDD, shows that three compounds are envisaged: the hydrated neodymium oxalate of $Nd_2C_6H_{20}O_{22}$ chemical formula, praseodymium hydrate ($Pr_5O_{30}.25H_20$), and iron-praseodymium oxide ($FeO_3Pr_{0.51}$).The NAA shows that the precipitate contains 86.27% of neodymium and 13.72% of praseodymium and impurities. The thermal decomposition of this precipitate is carried out in a furnace (900°C, 1H) according to the reaction (a):

$$Nd_2(C_2O_4)_310H_2 \rightarrow Nd_2O_3 + 6CO_2 + 10H_2O \quad (a)$$

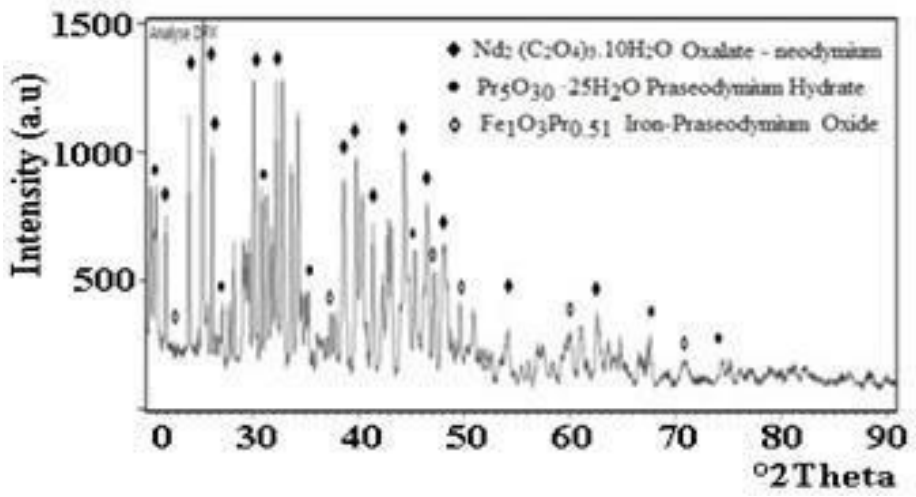

Figure 7: *XRD pattern for the neodymium oxalate*

The result of chemical composition analysis for Nd_2O_3 is in accord with XRD pattern (Figure 8), in which the oxide of neodymium phase (hexagonal) is observed. The spectrum shows three intense peaks corresponding to the diffraction of the plans (110), (102) and (103). The presence of $PrNdO_4$ was also confirmed.

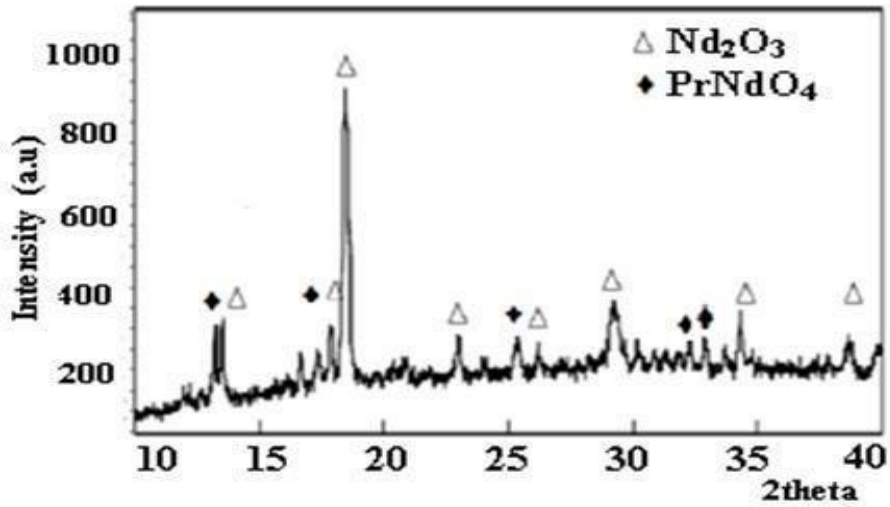

Figure 8: *XRD pattern for the neodymium oxide*

The last step is the reduction at 750°C of both oxides obtained previously. The choice of a reducer is conditioned initially by thermodynamic considerations resulting from the diagram of Ellingham, but also for kinetic and economic considerations. We chose CaCl2 in the presence of sodium according to reaction (b,c):

$$Nd_2O_3 + 3CaCl_2 + 6Na \rightarrow 3CaO + 2Nd + 6NaCl \quad (b)$$

$$PrNdO_4 + 4CaCl_2 + 8Na \rightarrow 4CaO + PrNd + 8NaCl \quad (c)$$

The consideration of the diagrams of Ellingham is by the way when the difficulty of the reduction of oxides arises and in particular of metallic oxides in order to extract the elements. By taking into account the number of components, phases and equilibrium relations, the use of Gibbs phase rule gives a variance v =1, therefore we have an invariant system. The control of the temperature is sufficient. After reduction the product obtained is analyzed by XRD. The results are given in (Figure 9). The XRD spectrum of the obtained product shows the presence of CaO, Nd, NdPr and NaCl. Three intense peaks of neodymium, assigned to the diffraction of the planes (111), (200) and (220), corresponding to cubic structure and alattice parameter of 0.48 nm.

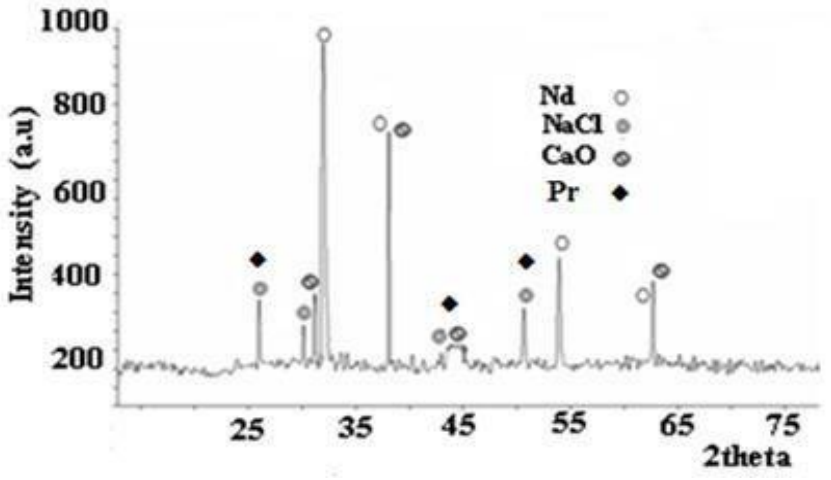

Figure 9: *XRD pattern reduction of neodymium oxid*

4. Conclusion

For the determination of impurities in trace, neutron activation analysis is one of the few methods that achieve its theoretical limits of detection. His response times are dependent on the decay period of radioisotopes used and can reach several days. We have shown that this method can analyze trace and ultra-trace. From the same sample NAA gives us the ability to assay simultaneously a large number of elements present in the Nd-Fe-B alloy used as a super magnet.

5. Acknowledgment

We acknowledge financial support from the Research Thematic Agency in Science and Technology. The authors are grateful for ATRST Algiers, Algeria.

References

B. Mokili & C. Potrenaud. (1996). Modelling of the extraction of Nd and Pr nitrates from aqueous solutions containing a salting-out agent or nitric acid by tri-n-butyl phosphate. Journal of Solvent Extraction and Ion Exchange. 14(4) pp617.

C. DE Wispelaere, J. P. OP DE Beeck & J. Hoste. (1973). non-destructive determination of trace impurities in iron by thermal neutron activation analysis with long – LIVED ISOTOPES, Institute of Nuclear Sciences, Ghent University, Ghent, Journal of Analytica ChiraicaActa. 64 pp321-332.

C.Milmo (2010) Concern as China clamps down on rare earth exports, 318.

G.A. Moldoveanu & V.G. Papangelakis, (2012). Recovery of rare earth elements adsorbedon clay minerals I. Desorption mechanism, Hydrometallurgy. 117–118, pp 71–78.168.http://dx.doi.org/10.1016/j.hydromet.2012.02.007

J.H. Rademaker, R. Kleijn & Y.X. Yang, (2013). Recycling as a strategy against rare earth element criticality: a systemic evaluation of the potential yield of NdFeB magnet recycling, journal of Environ. Sci. Technol. 47pp10129–10136.http://dx.doi. org/ 10. 1021/es305007w

J.W. Lyman & G.R. Palmer. (2011). Recycling of rare earths and iron from NdFeB magnet scrap, Journal of High Temperature Materials and Processes. 11(1–4)pp175.

M. Zakotnik, I.R. Harris & A.J. Williams. (2007). Possible methods of recycling NdFeB-type

sintered magnets using the HD/degassing process, Department of Metallurgy and Materials, University of Birmingham 450 pp 525–53.

M. Zakotnik, I.R. Harris & A.J. Williams. (2008). Multiple recycling of NdFeB-type sintered magnets, Journal of Alloys and Compounds [online]. 469.pp.314–321.Available http://www.sciencedirect.com.www.sndl1.arn.dz/science.

S. Ruoho, Modeling Demagnetization of Sintered NdFeB Magnet Material in Time-Discretized Finite Element Analysis, Department of Electrical Engineering, Aug. 1, 2011.

S. Lalleman, M.Bertrand & E.Plasari, (2011). Physical simulation of precipitation of radioactive element oxalates by using the harmless neodymium oxalate for studying the agglomeration phenomena, Journal of Crystal Growth. 342 pp42–49.

S. Itakura, R. Sasai & H. Itoh. (2005).Resource recovery from Nd–Fe–B sintered magnet by hydrothermal treatment, Journal of Alloys and Compounds, 408–412 pp1382–1385.

T. Saito, H. Sato & T. Motegi, (2006). Recovery of rare earths from sludges containing rare-earth elements, Journal of Alloys and Compounds, 425pp145–147.

T. H. Okabe, O. Takeda, K. Fukuda & Y. Umetsu, (2003). Direct extraction and recovery of neodymium metal from magnet scrap, Journal of Materials Transactions [online] 44(4) pp 798. Available http://dx.doi.org/10.2320/matertrans.44.798.http://dx.doi.org /10.2 320/ matertrans.44.798

T. Kobayashi, Y.Morita & M.Kubota, (1988). Development of Partitioning Method:Method of Precipitation Transuranium Elements with Oxalic acid", JAERI-M88 pp 026.

W. Yantasee, et al., (2009). Selective removal of lanthanides from natural waters, acidic streams and dialysate. Journal of Hazard Mater. 168 pp 1233–1238.http://dx.doi. org/10. 101 6/j.jhazmat.2009.03.004

W H. Duan, P J.Cao & Y J.Zhu. (2010). Extraction of rare earth elements from their oxides using organophosphorus reagent complexes with HNO_3 and H_2O in supercritical CO_2. Journal of Rare Earths. 28(2) pp 221. http://dx.doi.org/10.1016/S1002-0721(09)60084-3

X Y.Du & T E.Graedel. (2011). Global rare earth in-use stocks in NdFeB permanentmagnets. Journal of. Ind. Ecol, (15) pp 836.

Y. Kanazawa & M. Kamitani, (2006). Rare earth minerals and resources in the world, Journal of Alloys and Compounds. 408–412pp 1339–1343.